Collinear Setup for Two-Color High-Harmonic Generation

Bachelor thesis
by
Rimantas Budriūnas

Supervisor: Cord Arnold

LUND UNIVERSITY

Abstract

High harmonic generation (HHG) is a process in which extremely short bursts of coherent ultraviolet/soft x-ray radiation are generated by firing intense laser pulses into a dilute gas. During the long history of high harmonic generation research, several improvement schemes have been proposed. One of them was to use the driving laser pulse along with its second harmonic, which was found to raise generation efficiency and to enhance certain parameters of the harmonic radiation. This improved method is known as two-color high harmonic generation.

Two-color high harmonic generation requires precise control over the polarizations of the pulses and the time delay between them. At the Lund High Power Laser Facility this was previously done by using a two-color interferometric setup which was tedious to align and it required major changes to the HHG setup to switch between normal and two-color HHG. The aim of this work was to design, construct and test a collinear optical system that would allow transforming a high harmonic generation experiment into a two-color high harmonic generation experiment quickly and with minimum effort.Within the course of the project, types of optical components adequate for such a system were identified. After performing numerical simulations of the optical properties of the system, optimal component parameters were chosen. The compact system was assembled and tested.

Contents

Supervisor: Cord Arnold
Lund, January 2013

List of abbreviations

BBO Beta Barium Borate, a crystal used for nonlinear laser frequency conversion

FS Fused silica, a type of glass notable for low nonlinear pulse distortions

HHG High harmonic generation

KDP Potassium Dihydrogen Phosphate, another crystal used for nonlinear laser frequency conversion

MBES Magnetic Bottle Electron Spectrometer

SH(G) Second harmonic (generation)

Chapter 1

Introduction and aim of work

High harmonic generation (HHG) is a nonlinear optical process when extremely short bursts of ultraviolet/soft x-ray radiation are generated by firing intense laser pulses into a dilute gas. In contrast to the usual perturbative optical harmonic generation, where the generated harmonic intensity drops rapidly with increasing harmonic order, the spectrum of HHG light typically exhibits a plateau of harmonics with comparable intensities in the VUV/XUV range. HHG is one of only a few currently known methods of producing coherent radiation in this wavelength range.

During high harmonic generation, two harmonic pulses with opposite phases are normally generated every laser cycle, as illustrated schematically in figure 1.0.1a. In the spectral domain, only odd-numbered harmonics are generated, because both the gas and the laser pulse exhibit inversion symmetry. However, it has been shown that when a second harmonic (frequency doubled) field is added to the driving laser pulse, the symmetry is broken, and both odd and even harmonics are produced [1]. The broken symmetry also means that only one harmonic pulse is produced per laser cycle, which is desirable for stroboscopic applications. The overall efficiency of high harmonic generation is also enhanced. This process, referred to as $\omega + 2\omega$ high harmonic generation, is depicted schematically in figure 1.0.1b.

The aim of this work was to design, construct and test a compact, user-friendly optical system that would allow to transform a usual high-harmonic generation experiment into a $\omega + 2\omega$ high harmonic generation experiment with minimum effort.

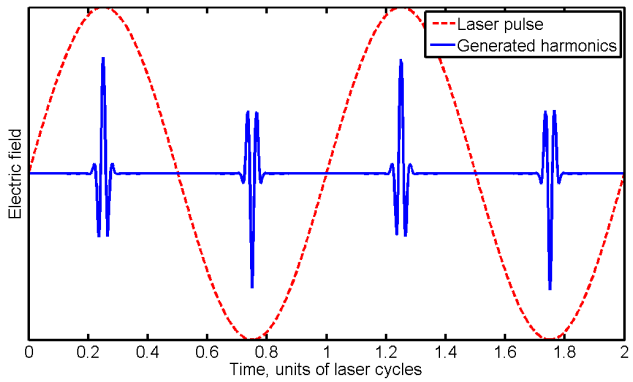

(a) High harmonic generation

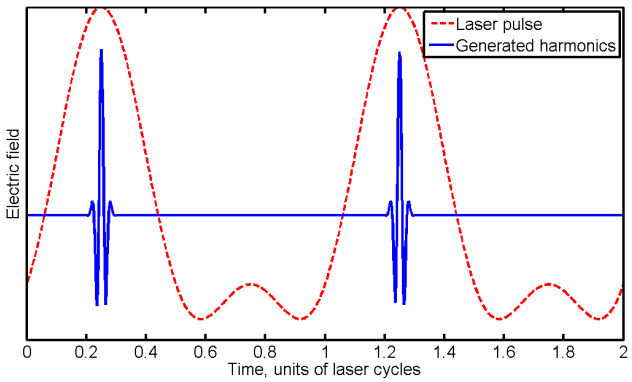

(b) High harmonic generation with second harmonic added to the driving laser pulse

Figure 1.0.1: Illustrations of the high harmonic generation process

Chapter 2

Design and Modeling

2.1 Analysis of the requirements

In order to find the best solution, the objective was broken down into smaller tasks. To be useful in a $\omega + 2\omega$ HHG experiment, the setup had to perform the following functions:

1. Generate the second harmonic of the input pulse, preferably so that the power of the generated second harmonic is at least 10% of the fundamental at output
2. Ensure that the fundamental pulse and the second harmonic have the same polarization[1]
3. Control the delay between fundamental and SH pulses, caused by material dispersion, so that the two pulses reach the target at the same time. The delay correction system should also allow continuous scanning of delay with sub-femtosecond resolution
4. Reduce or eliminate ellipticity of the output pulses, at least so that $\epsilon \equiv P_y / P_x \leq 0.01$

The tasks are summarized in fig. 2.1.1. In the figure and throughout the rest of the paper, the coordinate axes are arbitrarily selected so that the laser pulses propagate along the z axis and the input laser pulse is polarized along the y axis.

Besides formally performing the basic functions, some of the qualities one would like an apparatus like this to possess are:

1. High throughput, so that as little light is lost in the process as possible
2. Ease of operation
3. Compactness
4. Low dispersive broadening of the laser pulses

It is to be noted that the setup is designed to operate with the Ti:Sapphire laser system in the Attosecond Laboratory of Lund Laser Centre. At the time of writing, the nominal laser parameters are as follows: pulse duration FWHM $\tau_{FWHM} \approx$ 20fs; a Super-Gaussian spectrum with 750nm $< \lambda <$ 850nm; repetition rate $f_{rep} =$ 1kHz. About 4mJ of pulse energy is available for this particular experiment. The $\omega + 2\omega$ setup will be used in the pump arm of a pump-probe interferometer and will thus receive about 70% of the full 4mJ pulse energy.

In the following few paragraphs, it will be analyzed how the aforementioned functions could be performed in a practical device and what results could be expected using realistic components.

2.2 Second harmonic generation crystal

The choice of the second harmonic generation crystal involves selecting the right material, phase matching angle and thickness. For this application, the choice of material type was straightforward. Of currently known and widely available nonlinear crystals, β-Barium Borate (BBO) is superior to other types of crystals because of its high nonlinear susceptibility, which directly means better SHG efficiency for a given intensity. Furthermore, these crystals can be grown to various sizes, including thin wafers for broadband applications. If a very large crystal was required, it may have been wiser to choose Potassium Dihydrogen Phosphate (KDP), however, this was not an issue in our case.

The next step is the choice of phase matching angle. SHG is an efficient process if and only if it is phase-matched, so that the input pulse and the SH pulse have the same phase velocities. In the case of Type I SHG and a negative uniaxial nonlinear crystal, the phase matching condition translates into

[1] There have been reports on two-color HHG experiments with fundamental and SH fields polarized orthogonally, notably [2, 3]. However, the presented HHG spectra exhibit large differences between intensities of odd and even harmonics, which were undesirable.

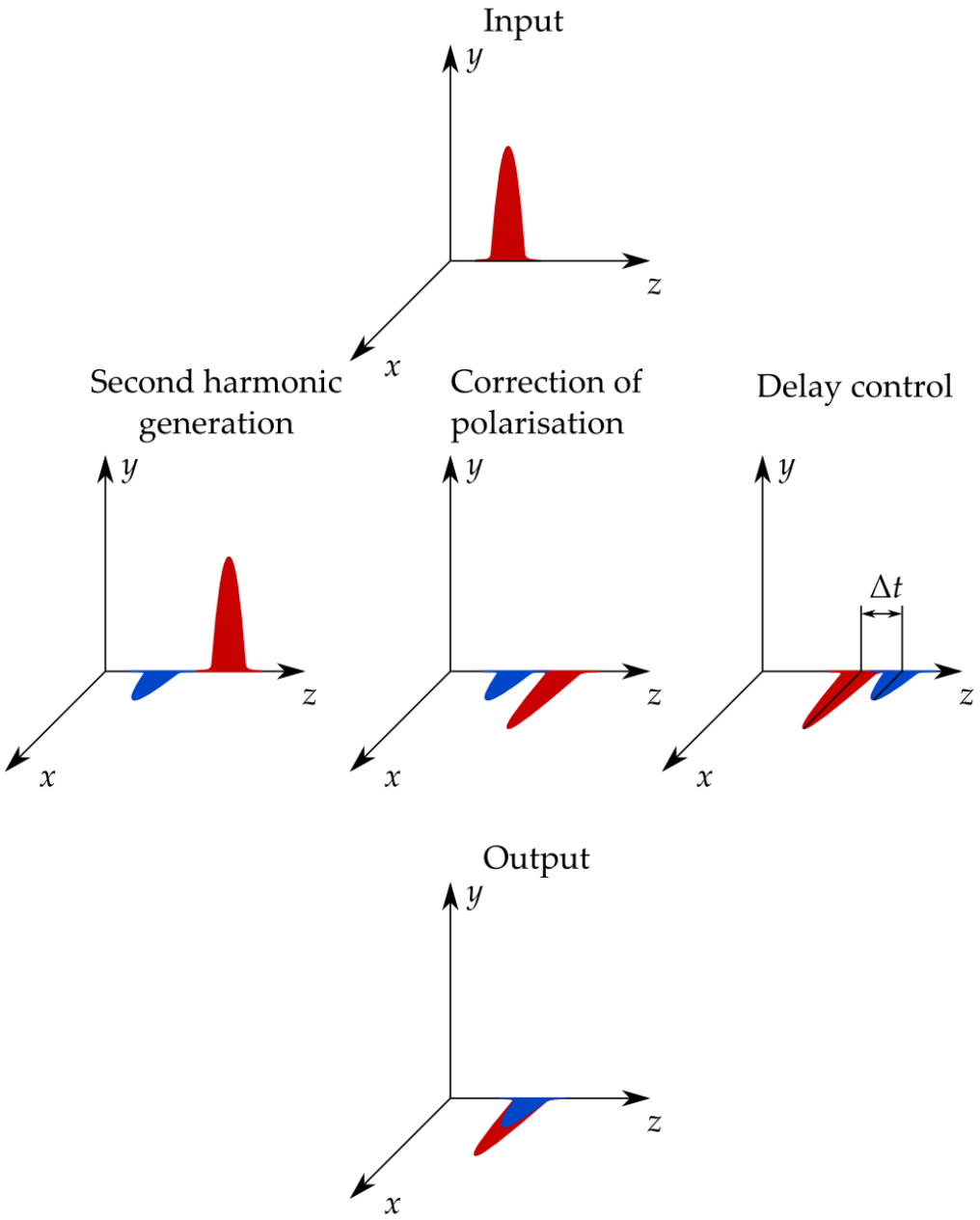

Figure 2.1.1: A summary of the functions the device must perform

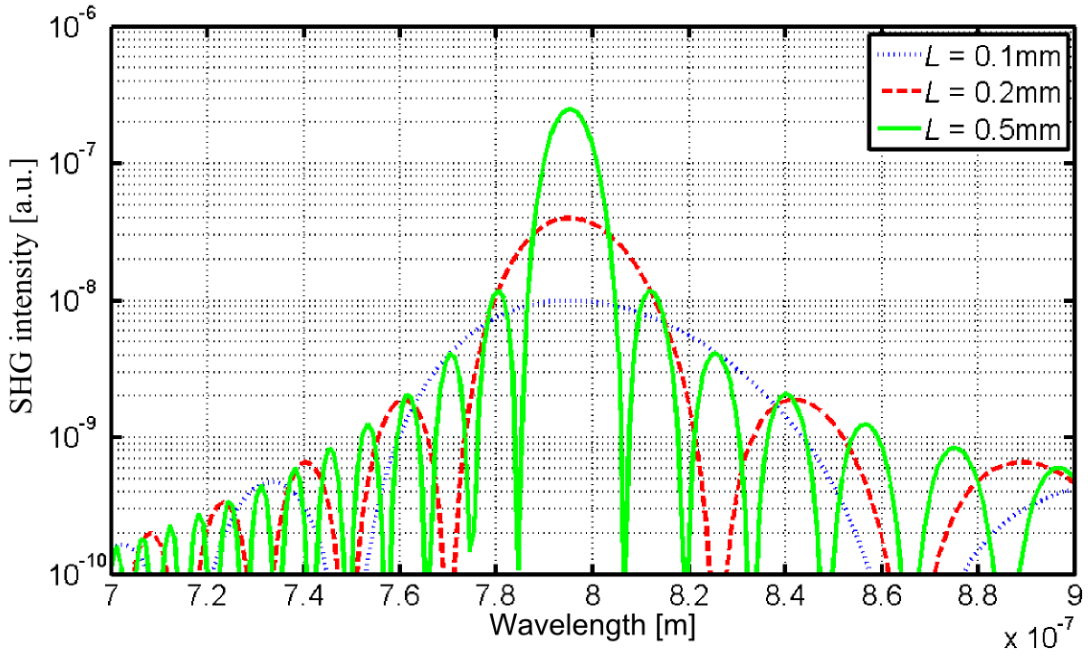

Figure 2.2.1: SHG intensity versus wavelength for different BBO crystal lengths

$$n_e(2\omega) = n_o(\omega)$$

where n_e and n_o are the frequency-dependent refractive indices for the extraordinary and ordinary rays in the nonlinear crystal, respectively. This is achieved by selecting a correct phase-matching angle θ, that is, an angle between the optical axis of the crystal and the wavevector of the incoming pulse. It is known from crystal optics [4] that the angle dependence of the refractive index can be expressed as

$$\frac{1}{n_e^2(\lambda,\theta)} = \frac{\cos^2(\theta)}{n_o^2(\lambda)} + \frac{\sin^2(\theta)}{n_e^2(\lambda,\theta=90^\circ)} \tag{2.2.1}$$

Using Sellmeier equations often provided by crystal vendors[2], the refractive indices n_e and n_o can be calculated for different wavelengths. The phase matching angle for frequency doubling $\sim$ 800nm radiation from a Ti:Sapphire laser turns out to be $\theta = 29.2^\circ$.

Perhaps the most delicate part is selecting the length L of the crystal. Theoretical analyses of the SHG process for the case of monochromatic waves show that the power of the generated second harmonic scales with L^2[5]. However, at least two factors put upper limits on L. First, because the input pulse is broadband, phase matching cannot be achieved for all of its spectral components. At least for monochromatic waves, SHG intensity is related to wavevector mismatch Δk as

$$I_{SHG} \sim L^2 \mathrm{sinc}^2\left(\frac{L\cdot\Delta k}{2}\right) \tag{2.2.2}$$

where

$$\Delta k = 2\pi\left[2\frac{n_o(\lambda)}{\lambda} - \frac{n_e\left(\frac{\lambda}{2},\theta\right)}{\frac{\lambda}{2}}\right]$$

Figure 2.2.1 shows eq. 2.2.2, plotted against wavelength for crystals of several different lengths.

It can be seen that while the intensity of the central peak grows significantly with increasing crystal length, the bandwidth narrows down quickly. The narrowed bandwidth means an increased duration of the SH pulse, which is tolerable up to some extent, but certainly not desirable.

Another upper limit on L is set by the group velocity mismatch length [6]. After propagating through a distance $L = L_{GVM}$, the fundamental and SH pulses separate in space and do not interact anymore. Group velocity mismatch length can be estimated as

$$L_{GVM} \approx \frac{\tau_{FWHM}}{\left|\frac{1}{v_g(\omega)} - \frac{1}{v_g(2\omega)}\right|}$$

In the case of frequency doubling a 20fs, 800nm pulse in BBO at $\theta = 29.2^\circ$, $L_{GVM} = 85.8\mu$m. However, 20fs is the absolute minimum pulse duration for the current laser system. As will be discussed later, it will be necessary to use

[2]For example, http://www.coherent.com/downloads/BBO_DS.pdf

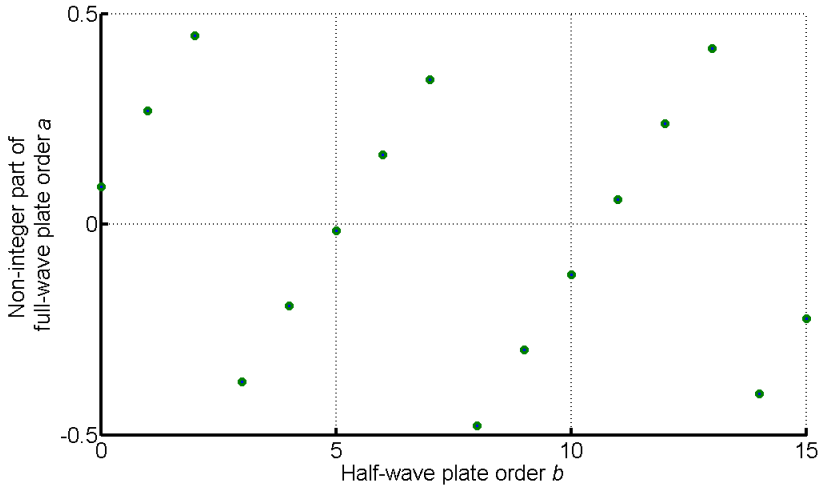

Figure 2.3.1: Deviations from integer values of the full-wave plate order for integer half-wave plate orders 0 to 15 calculated for crystalline quartz

a longer pulse at the input of the $\omega + 2\omega$ setup to keep output pulse duration low. It would be reasonable to expect an input pulse duration of 30-40fs, which would double the group velocity mismatch length.

In the end, a BBO crystal with a phase matching angle of 29.2° and thickness of 200μm was chosen.

2.3 Correcting the polarization

As defined in the requirements, the fundamental and the second harmonic pulses must be polarized parallel to each other. However, in Type I SHG, the second harmonic pulse is produced polarized perpendicularly to the fundamental pulse. While it would be simple to insert a half-wave plate into one arm of an interferometric setup, a special waveplate is necessary in the case of collinearly propagating fundamental and SH pulses. This way, it is necessary to keep the polarization state of one of the pulses intact, which requires the waveplate to operate as a full-order plate for this wavelength, and to rotate the polarization of the other pulse by 90 degrees, which means that the waveplate must be a half-wave plate for that wavelength. Mathematically, this is expressed as

$$\begin{cases} d\left[n_e\left(\lambda_1\right) - n_o\left(\lambda_1\right)\right] = a\lambda_1 \\ d\left[n_e\left(\lambda_2\right) - n_o\left(\lambda_2\right)\right] = \left(b + \frac{1}{2}\right)\lambda_2 \end{cases} \tag{2.3.1}$$

where d is the thickness of the birefringent material used for the waveplate, n_e and n_o are the extraordinary and ordinary refractive indices for particular wavelengths, and waveplate orders a and b are integer numbers. As seen, the waveplate will act as a full-wave plate (no effect on polarization) for λ_1 and as a half-wave plate for λ_2. Substituting for convenience $\Delta n\left(\lambda_i\right) \equiv n_e\left(\lambda_i\right) - n_o\left(\lambda_i\right)$, the equations in 2.3.1 can be rearranged to get

$$a = \left(b + \frac{1}{2}\right)\frac{\Delta n\left(\lambda_1\right)}{\Delta n\left(\lambda_2\right)}\frac{\lambda_2}{\lambda_1} \tag{2.3.2}$$

Once the waveplate orders are decided, eq. 2.3.1 can be rewritten to calculate the thickness of a chosen plate:

$$d = \frac{a\lambda_1 - \left(b + \frac{1}{2}\right)\lambda_2}{\Delta n\left(\lambda_1\right) - \Delta n\left(\lambda_2\right)} \tag{2.3.3}$$

Ideally, both a and b should be integers, which can only be approximated in reality due to material dispersion. As an example, fig. 2.3.1 shows how far a deviates from integer values if b values are chosen to be integers. For the calculation, the choice was made that $\lambda_2 = 800$nm (half-wave plate for the fundamental)[3]. As one of the most common waveplate materials, crystalline quartz was assumed. Once again, widely available Sellmeier equations provided by the waveplate manufacturers[4] were used to calculate the refractive indices n_e and n_o. For crystalline quartz, $\Delta n\left(400\text{nm}\right)/\Delta n\left(800\text{nm}\right) \approx 1.0896$ and consequently eq. 2.3.2 becomes $a = 2.1791b + 1.0896$.

It can be seen that most b values result in a values which are far from integers; for instance, if $b = 2$ was chosen, $a = 5.4478$ and such a plate would almost be a half-wave plate for both the fundamental and the second harmonic. Nevertheless, a few attractive combinations can be obtained. $b = 5$ would give $a = 11.9851$, which is very close to an integer value. It would be a really good option if the system was being designed for longer, narrow-bandwidth

[3]The nature of the calculations would not be affected in any way $\lambda_2 = 400$nm was chosen. However, better results are produced with $\lambda_2 = 400$nm.

[4]For instance, http://www.eksmaoptics.com/en/main/formulas/refractive

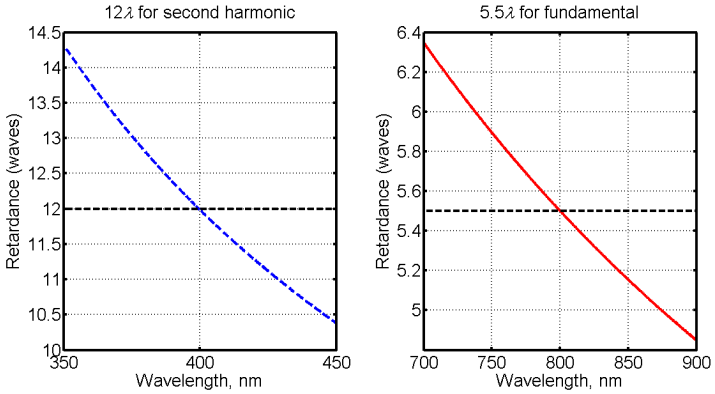

Figure 2.3.2: Retardation as a function of wavelength for a 5-th order $\lambda/2$ waveplate

pulses. However, it is known that a waveplate's bandwidth narrows sharply with increasing waveplate order. Because the setup is intended to be used for 20fs pulses with a bandwidth of ~100nm at ~800nm, this is not an option; the second best option is then $b = 0$; $a = 1.0896$. The retardation the pulses would experience after propagating through a waveplate with $b = 5$ and $a = 11.9851$ are shown in fig. 2.3.2

It is clear that such a waveplate would only work for a very narrow wavelength range, since the retardation varies strongly with wavelength. For a birefringent retarder of thickness d, obtained from eq. 2.3.3, the actual transmission efficiency can be calculated using Jones calculus [7]. For the incoming fundamental pulse, polarized along the y direction,

$$\begin{bmatrix} T_x(\lambda_F) \\ T_y(\lambda_F) \end{bmatrix} = \left| R(45^\circ) \times \begin{bmatrix} \exp\left\{2\pi i \cdot \frac{d \cdot n_o(\lambda_F)}{\lambda_F}\right\} & 0 \\ 0 & \exp\left\{2\pi i \cdot \frac{d \cdot n_e(\lambda_F)}{\lambda_F}\right\} \end{bmatrix} \times R(-45^\circ) \times \begin{bmatrix} 0 \\ 1 \end{bmatrix} \right|^2$$

while for the second harmonic, initially polarized along the x axis,

$$\begin{bmatrix} T_x(\lambda_{SH}) \\ T_y(\lambda_{SH}) \end{bmatrix} = \left| R(45^\circ) \times \begin{bmatrix} \exp\left\{2\pi i \cdot \frac{d \cdot n_o(\lambda_{SH})}{\lambda_{SH}}\right\} & 0 \\ 0 & \exp\left\{2\pi i \cdot \frac{d \cdot n_e(\lambda_{SH})}{\lambda_{SH}}\right\} \end{bmatrix} \times R(-45^\circ) \times \begin{bmatrix} 1 \\ 0 \end{bmatrix} \right|^2$$

where $T_{x,y}$ are power transmission coefficients for x and y-polarized light, and $R(\alpha) = \begin{bmatrix} \cos\alpha & -\sin\alpha \\ \sin\alpha & \cos\alpha \end{bmatrix}$ is the coordinate rotation matrix used to account for the fact that the ordinary and the extraordinary directions of the waveplate must be oriented at 45° with respect to the lab coordinates in order for the half-wave plate to rotate the polarization of the fundamental pulse by 90°. The calculated transmission to the desired polarization, T_x, is shown in fig. 2.3.3 for the $b = 5$ waveplate.

Equivalent data for the zero-order half-wave plate are given in figures 2.3.4 and 2.3.5.

While the transmission peak in the SH spectral region is somewhat offset from the desired value of 400nm, the overall transmission is obviously much better: at worst, only a few percent of the fundamental pulse and no more than 20% of the second harmonic pulse are transferred to the wrong polarization. Thus, the zero-order waveplate is clearly a better choice. Returning to eq. 2.3.3, one can calculate that the thickness of such a waveplate made of crystalline quartz must be $d \approx 44.9\mu$m. Such thin waveplates cannot be produced practically. However, it is still possible to achieve a „fake" zero-order waveplate by using two thicker pieces of quartz with a thickness difference equal to d and orienting them so that the extraordinary axis of the first plate is aligned with the ordinary axis of the second plate. Assuming that the ordinary axis of the first piece is oriented along the x axis, making the extraordinary one oriented along the y axis, and the axes of the second quartz piece are rotated 90°, it is readily shown that the phase delays experienced by x- and y- polarized waves are in this case

$$\Phi_x = \frac{2\pi}{\lambda}\left[D_1 n_o + D_2 n_e\right]$$
$$\Phi_y = \frac{2\pi}{\lambda}\left[D_1 n_e + D_2 n_o\right]$$

where $D_1$and D_2 are the thicknesses of the two pieces. Allowing $D_1 - D_2 = d$ and again substituting $\Delta n = n_o - n_e$, the retardance difference $\Delta\Phi = \Phi_x - \Phi_y$ is found to be

$$\Delta\Phi = \frac{2\pi}{\lambda}\left[D_1(n_o - n_e) + D_2(n_e - n_o)\right] = \frac{2\pi}{\lambda}\left[D_1\Delta n - D_2\Delta n\right] = \frac{2\pi}{\lambda} d\Delta n$$

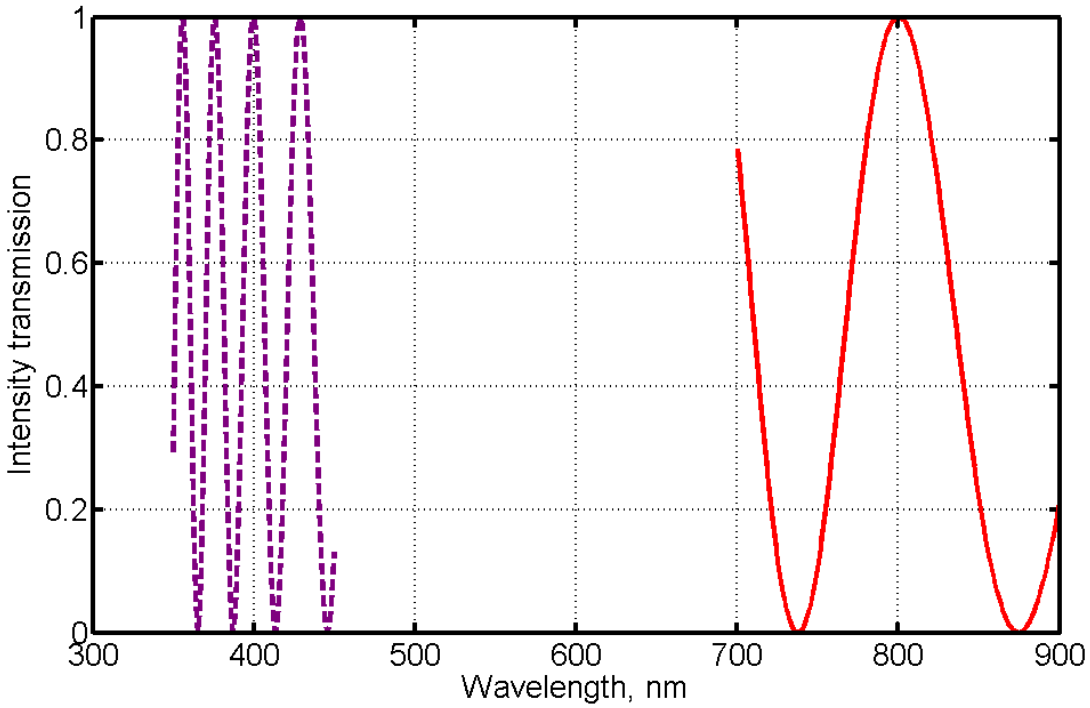

Figure 2.3.3: Spectral transmission to the desired polarization direction when using a 5.5λ waveplate

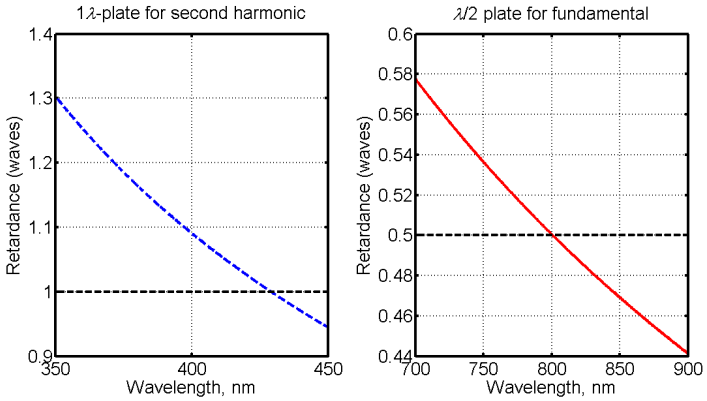

Figure 2.3.4: Retardation as a function of wavelength for the zero-order $\lambda/2$ waveplate

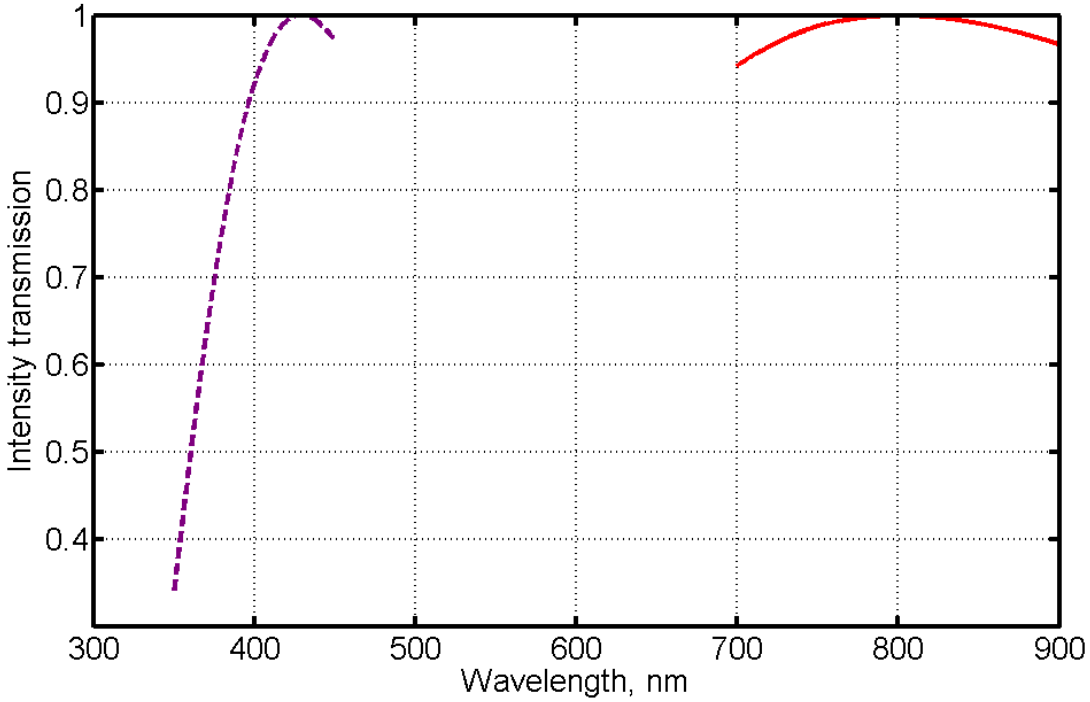

Figure 2.3.5: Spectral transmission to the desired polarization direction when using a 0.5λ waveplate

Table 2.1: Polarizer types

Type	Polarizing wavelength range	Extinction ratio	Transmission efficiency	Dispersion
Thin film[5]	$<$ 100nm around a design wavelength	1 : 15	$<$ 96%	Low
Birefringent (Glan-Thompson, Glan-Taylor)	300nm – 2300nm	$> 1 \times 10^5$	$\approx$ 95%	Very high
Ultrabroadband wire grid	350nm – 2600nm	$> 1 : 2 \times 10^3$ at 400nm $> 1 : 10^4$ at 800nm	$<$ 85%	Medium
1 Brewster plate	300nm – 1000nm	$\approx 1 : 1.35$	$\approx$ 100%	Very low
10 Brewster plates	300nm – 1000nm	$\approx 1 : 20$	$\approx$ 100%	Low

As one can see, the retardance difference, which decides the type of the waveplate, is only determined by the thickness difference. Thus, there is no need for very thin quartz plates - a zero-order waveplate can be produced from two quartz pieces of any thicknesses, as long as their thicknesses differ by the required value.

In the end, a waveplate very similar to the zero-order waveplate described above was ordered from Eksma Optics.

2.4 Cleaning the polarization

Considering the spectral width of the pulses the device is supposed to work with, it is unreasonable to expect any kind of waveplate to work ideally for the whole spectral range of the input pulses. Having estimated the transmission efficiencies to the desired (x) polarization and undesired (y) polarization, the next question is, how to remove the y-polarized field.

Although polarizers are very common in laser optics, the task is not trivial in this case because of the extremely broad bandwidth required and the necessity to limit dispersive broadening of the pulses. This prohibits use of polarizers that would introduce large amounts of material into the beam path. Properties of various polarizer types are listed in table 2.1.

Thin dielectric film polarizers are perhaps the most commonly used polarizer type in ultrafast laser optics. However, we were not aware of any film polarizer capable of supporting the required bandwidth. Glan-Thompson and Glan-Taylor polarizers provide excellent bandwidth and extinction ratio, but introduce much more dispersion than acceptable as they are made of birefringent prisms which add at least about 1cm of dispersive material to the beam path. A wire grid polarizer may be a solution, but the losses are generally unacceptable.

The actual solution came from considering polarization by reflection. It is known that if light falls onto an interface of two transparent materials at a certain angle, known as Brewster's angle, light polarized normally to the interface

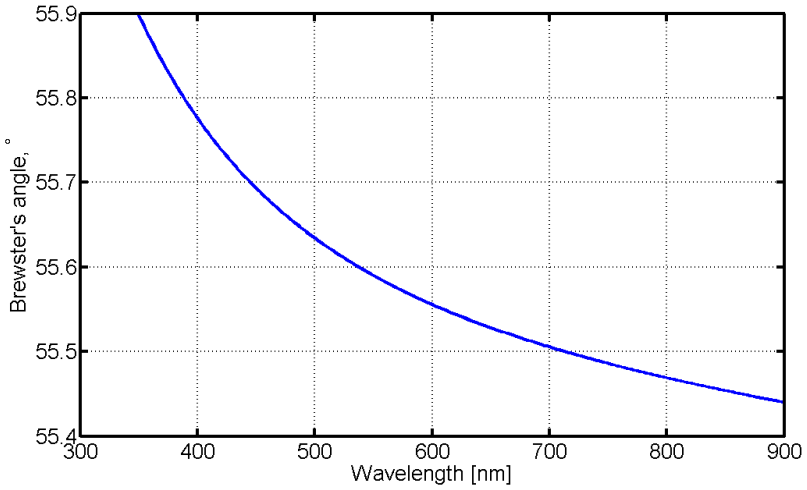

Figure 2.4.1: Brewster angles for different wavelengths. The interface is air-fused silica (FS) glass

(S-polarized) is transmitted without losses, while light polarized in the direction parallel to the interface (P-polarized) is partly reflected. This is because at Brewster's angle, the reflected beam would propagate at a right angle to the propagation direction of the transmitted beam. For S-polarized light, this would mean that the reflected wave must be a longitudinal electromagnetic wave, which does not occur in nature. As P-polarized light is partly reflected, while S-polarized light is transmitted without losses, transmitted light becomes more and more S-polarized with each interface it passes. Thus, the solution is to use several transparent plates oriented at Brewster's angle. The numerical value for Brewster's angle, when light falls onto a glass surface from air, is given by

$$\theta_B = \arctan\left(\frac{n_{glass}}{n_{air}}\right)$$

whereas n_{glass} and n_{air} are the refractive indices of glass and air, respectively. Naturally, Brewster's angle is wavelength-dependent because the refractive indices are. However, for an air-glass interface, the value varies very little, as shown in fig. 2.4.1. Thus, the bandwidth of such a polarizer can be extremely wide.

While the bandwidth is broad enough, such a polarizer only reflects about 14% of the unwanted light at each interface. Thus, to achieve the desired contrast $I_y/I_x \leq 0.01$, a number of reflections is required. Transmission and reflection were evaluated using the Fresnel equations

$$\begin{cases} R_S = \left(\frac{n_1\cos\alpha_1 - n_2\cos\alpha_2}{n_1\cos\alpha_1 + n_2\cos\alpha_2}\right)^2 \\ R_P = \left(\frac{n_1\cos\alpha_2 - n_2\cos\alpha_1}{n_1\cos\alpha_2 + n_2\cos\alpha_1}\right)^2 \end{cases}$$

$$\begin{cases} T_S = 1 - R_S \\ T_P = 1 - R_P \end{cases}$$

where $R_{S,P}$ and $T_{S,P}$ are the power transmission coefficients for S- (parallel to the interface) and P- (normal to the interface) polarized light, and α_1 and α_2 are the incidence and refraction angles.

Reflections from the air-glass and glass-air interfaces were considered. Modeling results for different numbers of uncoated FS plates are shown in figure 2.4.2.

On average, about 25% of the incoming light of unwanted polarization is transmitted when 5 FS plates are used. The transmission drops to about 15% for 7 plates and 6.5% for 10 plates. The light polarized in the right direction remains virtually unattenuated. While this may not a great contrast ratio for a polarizer, considering that only a few percent of the input light are transferred to the „wrong“ polarization by the waveplate to begin with, 10 or maybe even 7 glass pellicles seem to be adequate to keep ellipticity down to below 1%.

To minimize pulse distortion due to dispersion, ultrathin glass plates with a nominal thickness of 100µm were ordered, which would contribute at most 1.21mm of glass to the beam path at Brewster's angle, in the case of a polarizer made of 10 glass plates. This is superior to wire grid polarizers (>2.4mm) and highly superior to birefringent polarizers (>10mm). Fused silica glass was chosen over borosilicate glasses due to fused silica's lower nonlinearities.

2.5 Delay control

The two-color HHG experiment requires that the fundamental and the SH pulses arrive at the target simultaneously. While the method of delay control is obvious in an interferometric setup - the path is simply made longer for the faster pulse -, it is not as trivial for pulses propagating collinearly. The solution is to use a birefringent crystal after the SHG crystal, while the fundamental and SH pulses are still polarized orthogonally to each other. This way, the (normally

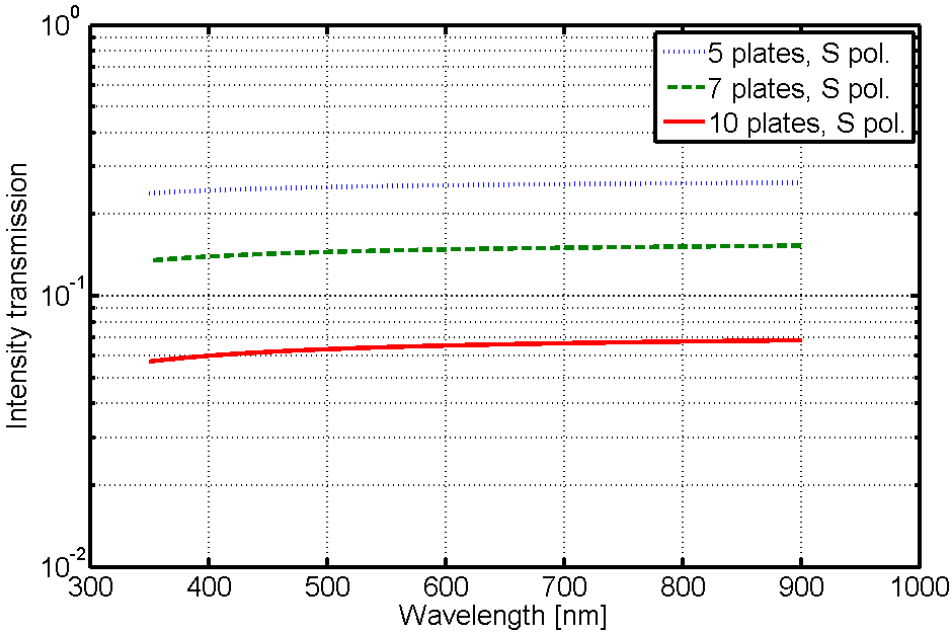

Figure 2.4.2: Attenuation of S-polarized light after passing through 5, 7 and 10 FS plates. The attenuation of x-polarized light was found to be too small to be taken into account

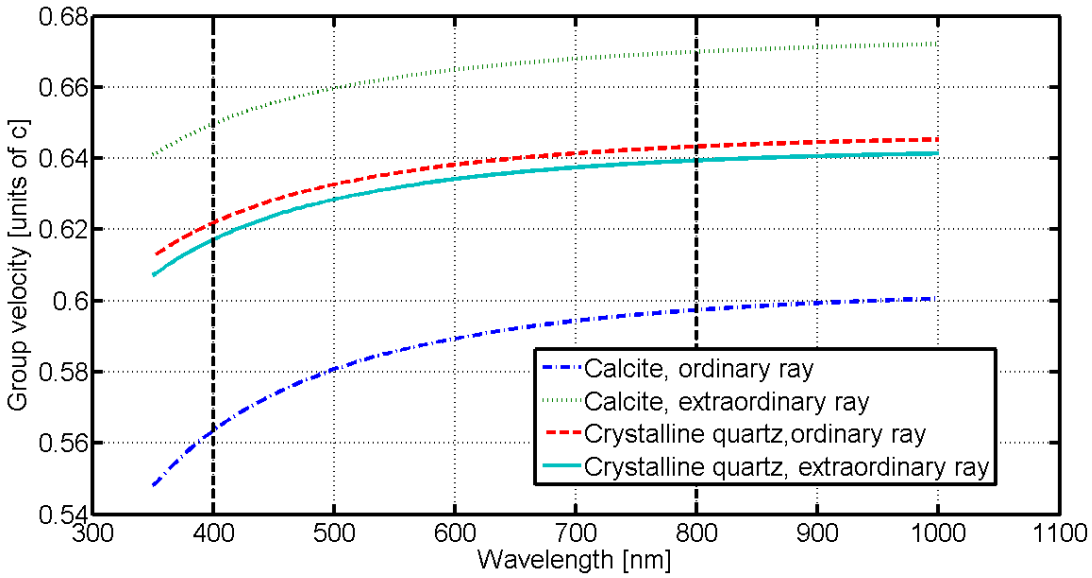

Figure 2.5.1: Group velocity dependence on wavelength in calcite and crystalline quartz

faster) fundamental pulse can be sent along the slow axis of the crystal, and the SH pulse can be propagated along the fast axis, compensating the delay.

Although the idea is simple, very few crystalline materials exist with birefringence strong enough to allow such an operation. In our case, the material of choice is calcite ($CaCO_3$). A plot showing the group velocities for the ordinary and extraordinary rays in calcite is given in fig. 2.5.1. The same dependence for crystalline quartz is given for comparison, showing that a blue pulse cannot be made faster than a red pulse in quartz, as is the case for most crystals[6].

To match the required delay, angle tuning is used. The ordinary axis of the crystal must be aligned with the polarization of the red pulse (y axis), and the extraordinary - with that of the blue pulse (x axis). Group delay compensation is then tuned by rotating the crystal around an axis parallel to the ordinary axis. This has two effects: first, the effective length of the crystal is changed; second, the angle between the wavevector and the optical axis is altered, affecting the effective refractive index for the extraordinary wave according to eq. 2.2.1.

Once the method is clear, it is necessary to calculate how much delay $\tau_{GVM} \equiv \tau\,(400\text{nm}) - \tau\,(800\text{nm})$ has to be compensated. With all the components decided upon, this is easily done by summing the delay differences experienced by the pulses:

[6]The only other material besides calcite with a possibility of $v_g\,(800\text{nm}) < v_g\,(400\text{nm})$ I am aware of is BBO. The birefringence of calcite is still stronger than that of BBO, allowing to use a thinner calcite plate, which is desirable.

Table 2.2: Group delays to be compensated

Dispersive component	Thickness/length	τ_{GVM_i}, fs
BBO crystal	0.2mm	37.73
Waveplate	1.88mm	344.26
1 FS wafer at Brewster's angle	0.1mm	18.80
Chamber window	0.3mm	46.62
Chamber window	0.5mm	77.70
Air	64cm	51.86

Table 2.3: Final list of components used in the $\omega + 2\omega$ HHG setup

Function	Component	Technical parameters
Second harmonic generation	BBO crystal	$d = 200\mu$m; $\theta = 29.2^\circ$
Delay compensation	Calcite plate	$d \approx 2.4$mm, $\theta \approx 54.9^\circ$, compensation range 420-650fs for incidence angles $-6^\circ < \alpha < 6^\circ$
Polarization correction	Crystalline quartz waveplate	$d \approx 1.88$mm; $\lambda/2$ for 800nm, $\approx 1 \cdot \lambda$ for 400nm
Polarization cleaning	5-10 Fused Silica wafers	$d = 100\mu$m (one wafer)

$$\tau_{GVM} = \sum_{i=1}^{n} d_i \left[\frac{1}{v_{g_i(400\text{nm})}} - \frac{1}{v_{g_i(800\text{nm})}} \right]$$

here the summation is performed over all the optical components in the system: the BBO crystal, the waveplate and the array of glass plates. Two less obvious „components" that must be accounted for are the entrance window to the vacuum chamber where the actual experiments are performed and the beam path in air, including both the distance through the $\omega + 2\omega$ setup and the path from the $\omega + 2\omega$ setup to the vacuum chamber (estimated to be about 64cm). The dispersion of air was calculated using equations from [8]. The calculated delay values for the different components are given in table 2.2. Two FS chamber windows are available in the lab, and it was not certain which would be used, so data are given for both of them.

The total τ_{GVM} varies between 574.48fs, when the chamber is fitted with the thinner window and the polarizer consists of 5 glass pieces, and 699.57fs, if the thicker chamber window is used and the polarizer is made of 10 FS wafers for a better extinction ratio.

A look at the optics market revealed that only a very limited selection of laser-grade calcite plates is available as standard products. In the end, a calcite plate about 2.4mm thick with a nominal delay compensation range of 420-650fs was chosen for lack of a better option. A little thicker plate or a plate with a different crystal cut angle would have been desirable, but proved difficult to obtain.

2.6 The final setup and estimation of dispersive pulse broadening

A technical description of the elements of the setup is listed in table 2.3. A schematic drawing of the device is shown in fig. 2.6.1, indicating the order of components, the polarizations of laser pulses and important angles.

While reliably estimating SHG efficiency is difficult, the expected transmission of all the other components is readily calculated by multiplying the transmission profiles obtained from calculations in the previous sections. The overall expected efficiency of the setup is given in figure 2.6.2. Expected ellipticity $\epsilon = I_y / I_x$ is shown alongside for polarizers composed of 5 and 10 FS plates. For 5 plates, ellipticity does not exceed 0.004 for the fundamental and 0.08 for the second harmonic. If 10 plates are used, ellipticity is further reduced to < 0.001 for the fundamental and < 0.02 for the second harmonic.

Finally, pulse shape distortion due to material dispersion must be analyzed. Dispersion means that different spectral components of a laser pulse travel at different phase velocities and therefore get dephased as the pulse propagates through dispersive media. As is usual in ultrafast laser physics, the spectral phase of the pulse is described by the coefficients of its Taylor expansion at a central frequency ω_0, namely

$$\Phi(\omega) = \Phi(\omega_0) + \frac{1}{1!} \frac{\partial \Phi}{\partial \omega}\bigg|_{\omega=\omega_0} \Omega + \frac{1}{2!} \frac{\partial^2 \Phi}{\partial \omega^2}\bigg|_{\omega=\omega_0} \Omega^2 + \frac{1}{3!} \frac{\partial^3 \Phi}{\partial \omega^3}\bigg|_{\omega=\omega_0} \Omega^3 + \frac{1}{4!} \frac{\partial^4 \Phi}{\partial \omega^4}\bigg|_{\omega=\omega_0} \Omega^4 + ... \tag{2.6.1}$$

where $\Omega \equiv \omega - \omega_0$. The derivatives in eq. 2.6.1 are referred to as group delay, group delay dispersion (GDD), third order dispersion (TOD), fourth order dispersion (FOD) and so on. Only the second and higher derivatives

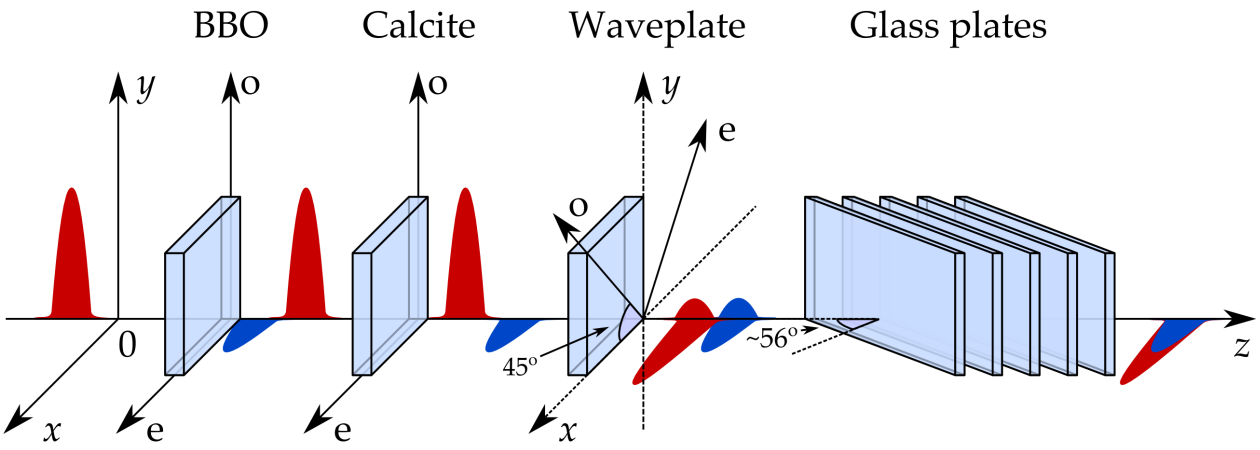

Figure 2.6.1: Schematic drawing of the final apparatus. Important alignment angles are indicated.

Table 2.4: 2nd, 3rd and 4th order dispersion introduced by the elements of the $\omega + 2\omega$ setup

Component	at 800nm			at 400nm		
	GDD, fs^2	TOD, fs^3	FOD, fs^4	GDD, fs^2	TOD, fs^3	FOD, fs^4
BBO crystal	14.36	10.20	-2.15	38.59	14.28	10.20
Calcite plate	184.39	128.37	-23.57	309.66	102.20	27.60
Waveplate	78.58	61.30	-22.96	218.36	69.62	15.69
Polarizer[7]	34.96	26.63	-11.12	94.44	29.29	6.34
Chamber window[8]	14.45	11.01	-4.56	39.03	12.10	2.62
Air	14.34	6.60	95.31	32.06	9.70	2.39
Total	341.09	244.075	59.89	732.15	237.19	54.12

have effects on the pulse shape, and for most optical materials, derivatives higher than the fourth are very small. Therefore, dispersion analysis is limited to GDD, TOD and FOD, which are given in table 2.4.

As could be expected, dispersion is far from negligible, as the combined thickness of the optical elements is over 5mm. It is also notable that the SH pulse experiences much stronger dispersion than the fundamental pulse. Distortion is obvious when the temporal shape of the fundamental pulse is modeled using inverse Fourier transform. The calculated pulse profile is shown in fig. 2.6.3 along with the minimum-duration, transform-limited profile. The broadened and distorted fundamental pulse would be of little use for HHG. However, the laser system in the laboratory includes an acoustooptic programmable dispersive filter, which enables one to shape the laser pulses almost arbitrarily. Thus, it would be simple to precompensate the dispersion of the fundamental pulse by adding equal but opposite amounts of GDD, TOD and FOD with the filter, so that a transform-limited pulse is obtained at output. However, this will certainly adversely affect SHG efficiency. It is also not straightforward to compensate the dispersion of the SH pulse. Optimum pulse shape settings will have to be determined experimentally to find a balance between SHG efficiency and good output pulse shape.

2.7 Mechanical components

Although the optical components are obviously the most important part of an optical device, the optics must be mounted conveniently and compactly. Thus, the mechanical components of an optical device must not be overlooked.

As has been shown in fig. 2.6.1, precision alignment of the optical axes of the birefringent crystals is needed. Thus, the three birefringent components must be mounted into holders that allow adjustment of not only tip and tilt, as provided by most standard optical mounts, but also rotation around an axis perpendicular to the surface of the components. A picture of the type of optical holder used in the setup is shown in figure 2.7.1. The holders were produced by Eksma Optics. Each holder is only about 28mm thick, which is useful in minimizing the size of the device.

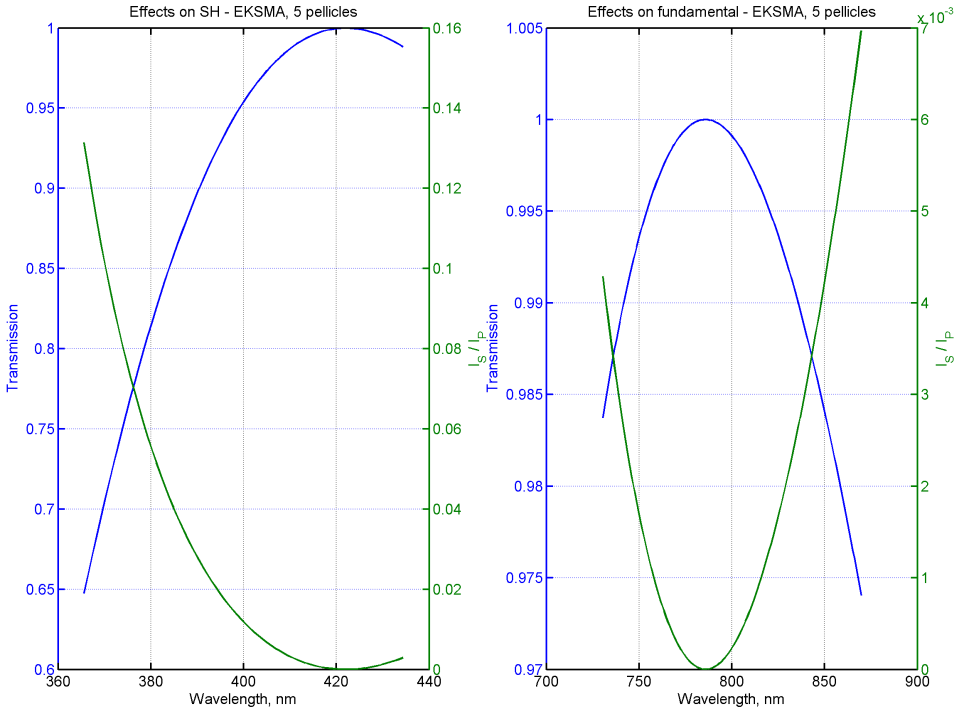

(a) Results with 5 glass plates used for the polarizer

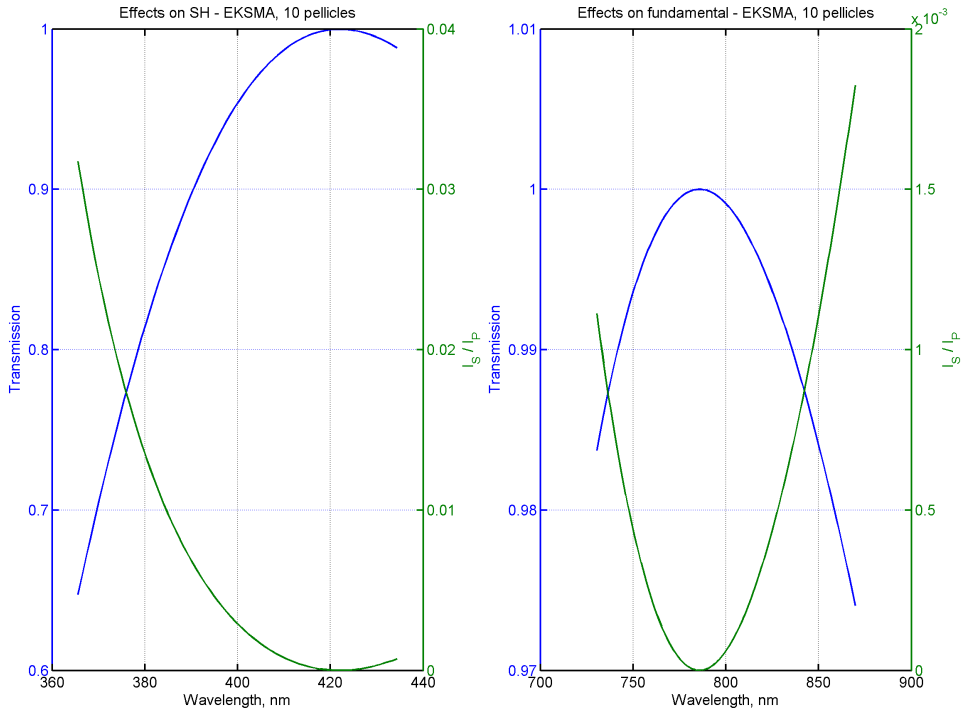

(b) Results with 10 glass plates used for the polarizer

Figure 2.6.2: Calculated spectral transmission and output pulse ellipticities for the whole setup. Losses due to reflections from the components were not taken into account

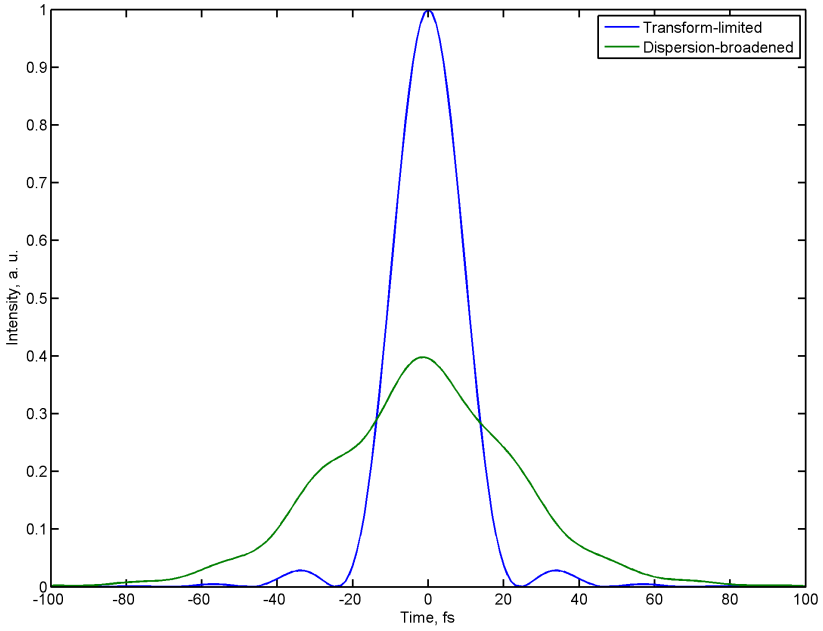

Figure 2.6.3: Comparison of transform-limited and distorted shapes of the fundamental pulse

Figure 2.7.1: Picture of the optical holder used for birefringent components of the $\omega + 2\omega$ HHG setup

The holder with the calcite plate was also mounted on a motorized rotation stage so that its angle can be controlled by a computer program. The rotation stage has a resolution of about 2.16 arc seconds, whereas the delay compensated by the calcite plate varies about 19fs per 1° of change of incidence angle. Thus, delay scans can be performed with a resolution of about 0.015fs.

The whole setup was fitted on a solid aluminum optical breadboard, measuring 25cm x 15cm. The width could still be made narrower by at least 5cm, but such a breadboard was unavailable.

Chapter 3

Alignment procedure

While the device is intended to be usable with no more effort from the experimenter than putting the assembled device into the beam and ensuring that the beam is sent in correctly, some initial calibration is required. The practical actions and additional equipment necessary to prepare the $\omega + 2\omega$ HHG setup for use are described below. Arrangement of components and equipment for each step of the procedure are shown in fig. 3.0.1.

3.1 Alignment of the BBO crystal

After the BBO crystal is setup to be vertical (usually done by), the important variable is the orientation of the crystal's axes with respect to the polarization of the input pulse. More precisely, the ordinary axis of the BBO crystal must be parallel to the polarization of the laser. The indication of correct alignment is a maximum of SHG efficiency. Thus, a red-blue beamsplitter and a power meter are required. The power of the SH beam is measured. The crystal must rotated in the holder to maximize that power. A possible layout is shown in fig. 3.0.1a.

For the most of the remaining alignment procedure, the presence of the second harmonic is likely to do more bad than good. Either the BBO crystal should be rotated by exactly 90 degrees, so that the laser pulse sees the extraordinary axis of BBO and no second harmonic is generated, or a blue-reflecting mirror should be placed right after the crystal for the next 2 or 3 steps.

3.2 Axes of the calcite plate

If absorbing polarizers are used for this part, as shown in fig. 3.0.1b, laser power should be turned down to a safe level. Reflective polarizers can, of course, be used as well.

Initially, the faces of calcite plate should be made parallel to the BBO crystal. Then, two polarizers should be inserted: one between the BBO and the calcite plate, set to allow y-polarized light, and one more after the calcite plate, transmitting x-polarized light. The calcite plate must be rotated so that a power meter placed after the red/blue beamsplitter registers no power.

The theory behind this procedure is illustrated in fig. 3.2.1. Figure 3.2.1a shows the initial polarization of the laser ($\vec{E}$) with reference to the lab coordinate system and an arbitrary alignment of the ordinary and extraordinary axes of the calcite crystal. Because the calcite plate has different refractive indices for the ordinary and extraordinary polarizations, the incoming laser pulse is split into two pulses, each polarized along one of the two principal directions (fig. 3.2.1b). The distribution of pulse energy between the o and e axes of the calcite is determined by the projections of $\vec{E}$ onto the o and e axes, as shown in fig. 3.2.1b. The ~2.4mm thick calcite plate introduces a delay of about 1.1ps between the two pulses. This is >50 times more than the pulse duration, so the pulses propagate separately and do not interact with each other to create an elliptical polarization, making the phase relation between the e and o pulses irrelevant. When the pulses reach the x-polarizer, the x-components of both $E_o$and E_e are transmitted, and the meter must show non-zero optical power (fig. 3.2.1c). However, if either the ordinary or extraordinary axis is matched to the input polarization (along the y axis, as in fig. 3.2.1d), no electric field along the x-axis is created.

(a) BBO crystal

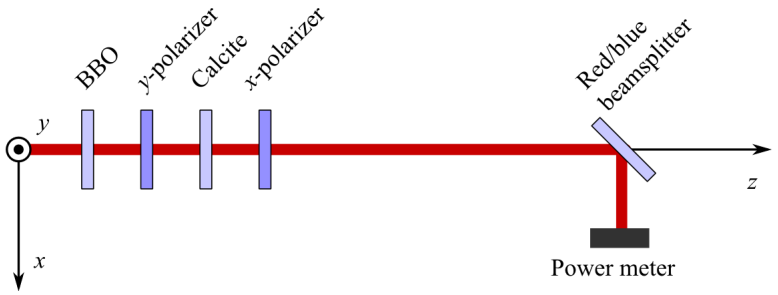

(b) Calcite plate

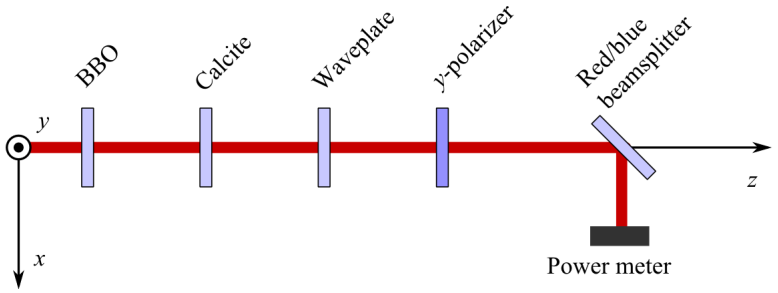

(c) Waveplate

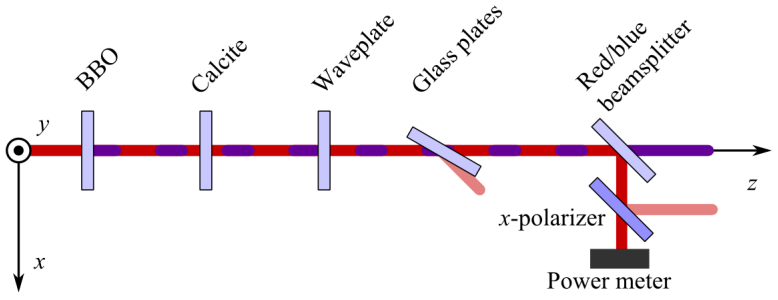

(d) Glass plate polarizer

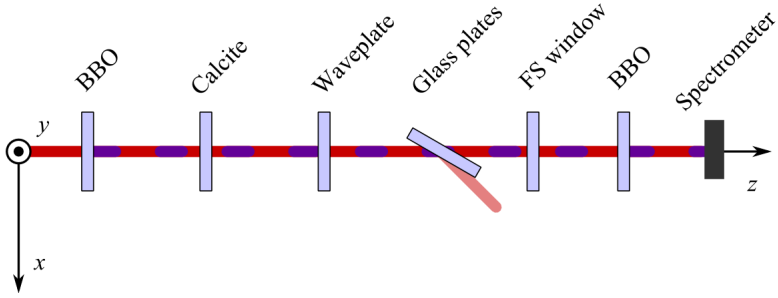

(e) Delay compensation

Figure 3.0.1: Different arrangements of optical equipment for the various steps of aligning the $\omega + 2\omega$ device

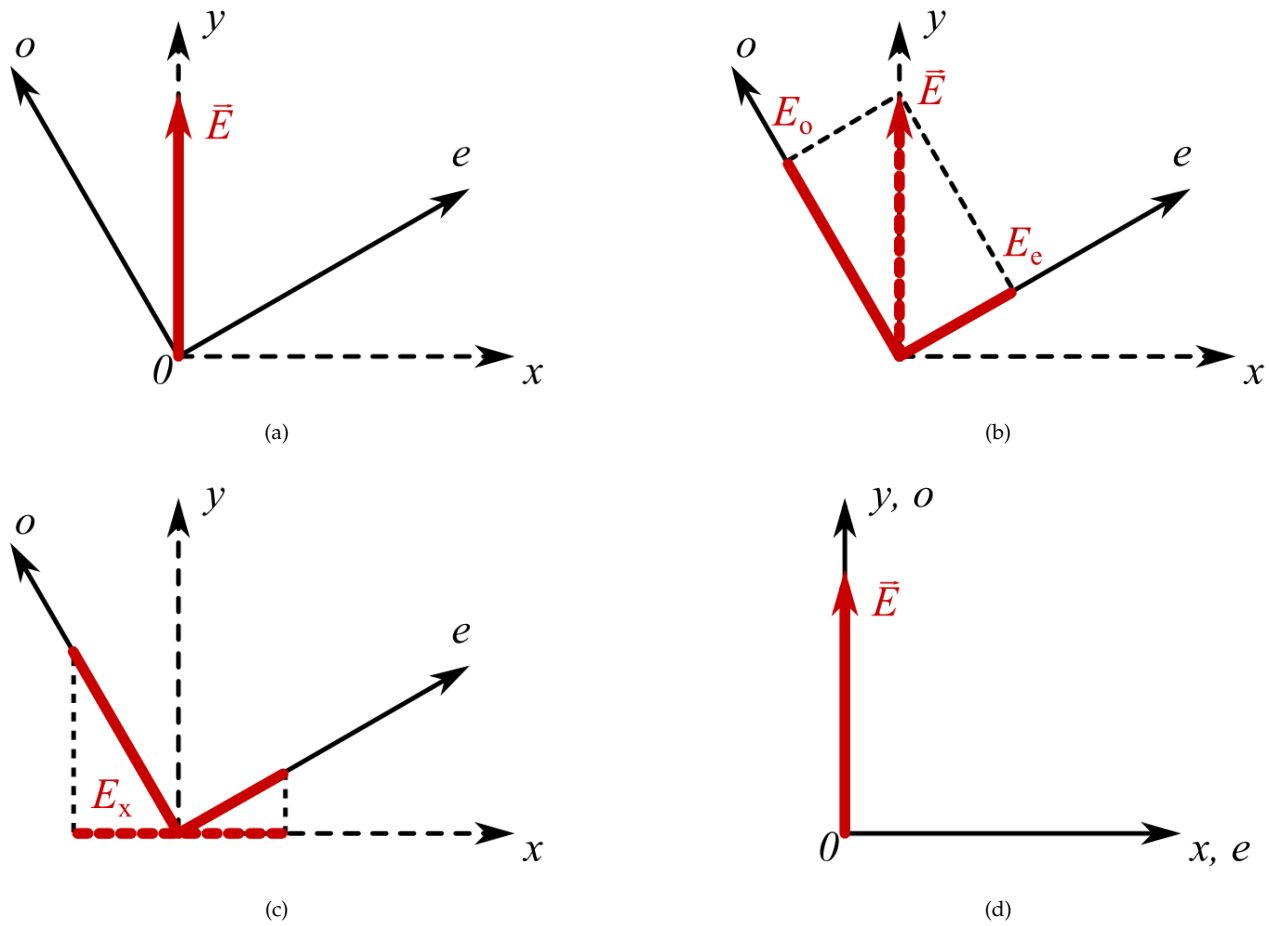

Figure 3.2.1: Alignment of the axes of the calcite plate

A drawback of the method described above is that it is ambiguous as one cannot distinguish if the extraordinary axis is aligned with the y axis, o with the x axis of the laboratory reference frame. For the operation of the device it is strictly necessary that the extraordinary axis be aligned with the x axis as otherwise the calcite plate will increase the delay between the red and the blue laser pulses instead of decreasing it, rendering the setup useless. However, even if the wrong axis is selected, it is still helpful because due to orthogonality of the o- and e- axes, a rotation of the plate by exactly 90 degrees is all it takes to correct the situation in case it turns out that it is impossible to compensate the interpulse delay caused by group velocity mismatch.

3.3 The waveplate

The alignment of the waveplate is a very standard procedure. A y-polarizer is placed after the waveplate, and the waveplate is rotated to get, once again, a minimum on the power meter. The arrangement is shown in fig. 3.0.1c. The waveplate could also be setup by rotating it so as to maximize throughput through the pellicle polarizer.

3.4 The polarizer

To find Brewster's angle, the arrangement shown in fig. 3.0.1d may be used. The angle of the glass plates should be adjusted to achieve maximum transmission of red light to x polarization.

If a broadband birefringent polarizer is available, a different arrangement could be used as well. In that case, the polarizer and power meter could be placed before the red/blue beamsplitter. Once again, the glass plates should be oriented to get maximum power. The benefit of using this arrangement would be that the power of both the fundamental and second harmonic is maximized, which means that an average of the Brewster angles for the fundamental and the SH pulses is found, whereas in the previous case Brewster angle is found for the fundamental only. However, the difference is very small.

3.5 Delay compensation

Once everything else is in place, the angle of the calcite plate must be adjusted to correct the necessary amount of group delay difference between the red and the blue pulses. This is best done by once again generating the second harmonic of the red pulse, this time at the output of the setup, and sending the blue pulses to a spectrometer. When the pulses are aligned correctly in time, spectral interference fringes should be observed in the spectrometer. The layout is shown in fig. 3.0.1e.

A little problem is that the red pulse and the initial blue pulse are now x-polarized, which means that the new blue pulse would be y-polarized if the second BBO crystal was aligned for maximum SHG efficiency. This way, if the SH pulses overlap in time, elliptical polarization will result, but spectral interference will not be observed. To correct for this, the second SHG crystal must be oriented off-axis, for instance, so that the ordinary axis makes a 45° angle to x or y axis, so that the second SH pulse has an electric field component parallel to the field of the first SH pulse.

Ideally, the second BBO crystal should be placed inside the vacuum chamber. Alternatively, a glass window can be inserted before the BBO crystal to account for the delay caused by the chamber window.

Chapter 4

Experimental testing

Tests were performed at the Attosecond Laboratory of Lund High Power Laser Facility. The device was assembled, aligned and high harmonics were generated in argon.

4.1 Characterization of the device

After the device was aligned as described previously, parameters important to the performance of the device were measured. The measurements were performed using a birefringent polarizer, a red/blue beamsplitter and two power meters for different power ranges. The results of fundamental and second harmonic power measurements and calculated ellipticities are given in table 4.1

The measurements indicate that the ratio of second harmonic and fundamental pulse powers $P_{SH}/P_F \approx 0.06$. While this is somewhat less than the desired $P_{SH}/P_F \approx 0.1$, it proved sufficient to achieve the desired HHG performance, as will be shown later.

Unfortunately, the accuracy of the measurements was severely limited by the fact that the beamsplitter did not split the red and blue beams completely - some blue leaked into the path of the red beam and vice versa. Furthermore, the beamsplitter does not work equally well for different polarizations. Thus, the measured power values are only approximate.

During the setup of the device, it was noticed that the ultrathin glass wafers used for the polarizer arrived dusty. Usual methods of cleaning optics proved to be of little use as the extreme thinness of the glass pieces makes it very difficult to handle them. It has been suggested that the glass wafers could be cleaned by washing them in a strong acid; however, there were no appropriate materials nor facilities available in the lab. Propagation through 7 dirty glass pieces proved to be destructive to beam quality, therefore the actual HHG experiments had to be performed without the polarizer.

4.2 High harmonic generation results

Even though the polarizer could not be used, the device was tested in a high harmonic generation experiment. The collinear $\omega + 2\omega$ setup was inserted into the path of a beam going to a vacuum chamber with a jet of argon gas. Although the appropriate angle of the calcite plate was found during alignment, the plate was first adjusted so that the red and blue pulses did not overlap in time. Then, the grating compressor of the laser system was adjusted to roughly precompensate the dispersion introduced by the setup, so that a good HHG signal was obtained. When the temporal overlap was restored, even harmonics appeared in the spectrum recorded by a magnetic bottle electron spectrometer, shown in fig. 4.2.1. It is difficult to directly compare HHG efficiency with and without the setup as some other experimental parameters were varied, but it can be stated that generally no strong reduction in the signal was noticed.

It is known that in two-color HHG the intensities of odd and even harmonics are strongly dependent on the relative phase of the fundamental and SH pulses [9]. Thus, the logical next step was to scan the red-to-blue pulse delay by rotating the calcite plate. The results are given in fig. 4.2.2.

Table 4.1: Device performance characteristics

Wavelength	Power in x-polarization P_x, mW		Power in y-polarization P_y, mW		Ellipticity P_y/P_x, %	
	No polarizer	7 FS plates	No polarizer	7 FS plates	No polarizer	7 FS plates
800nm	910	910	25.3	9.2	2.78	1.01
400nm	55	52.7	3	0.46	5.45	0.87
800nm+400nm	950	950	30.8	10.6	3.24	1.12

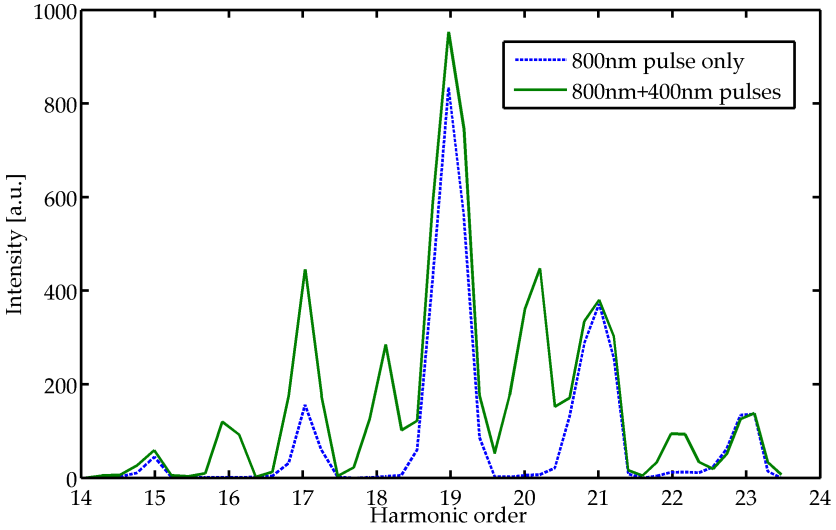

Figure 4.2.1: High harmonics spectra measured with a magnetic bottle electron spectrometer

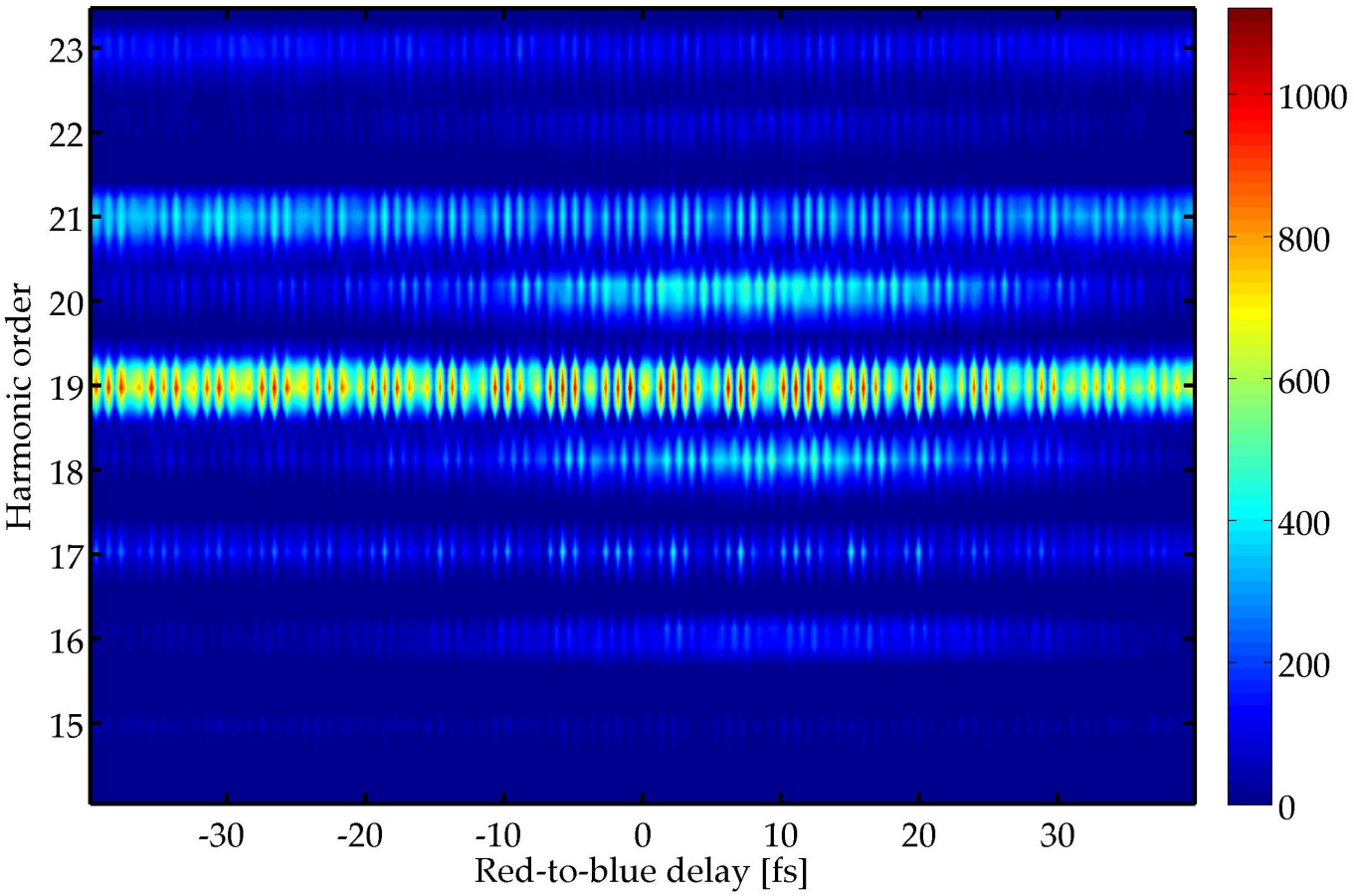

Figure 4.2.2: Variation of high harmonics spectra when the delay between the fundamental and second harmonic pulses is scanned. Color code shows photoelectron counts

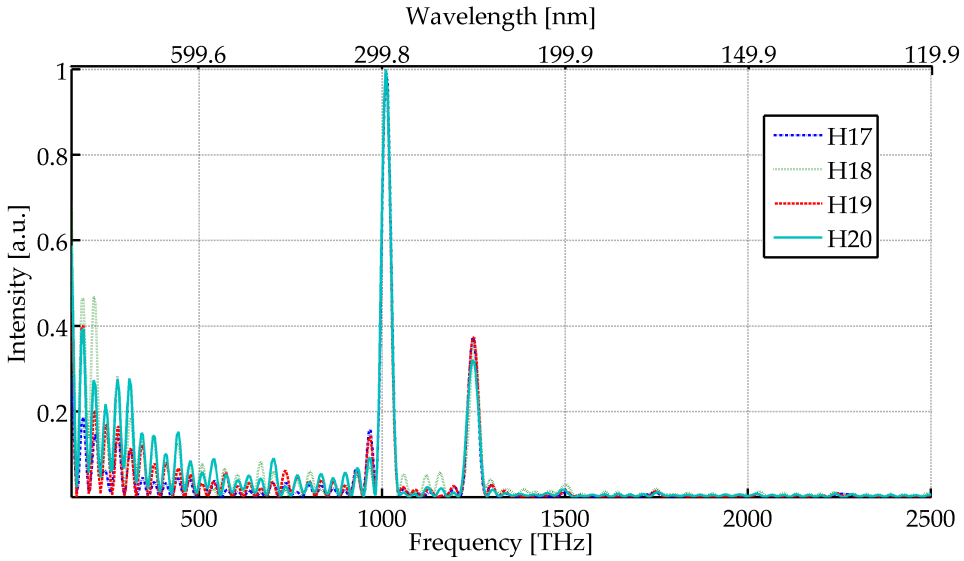

Figure 4.2.3: Frequency spectra of intensity oscillations for harmonics 17 to 20

The intensities of harmonics oscillate when the delay is scanned. Although these oscillations could be expected to have a frequency equal to the carrier frequency of the SH pulse, this is not the case here. It can be noted that the oscillations are composed of more than one frequency because beats are visible in the image. Oscillation spectra for harmonics 17 to 20 are given in fig. 4.2.3.

Intensities of all observed harmonics oscillate at very similar frequencies. It can be seen that the beats in fig. 4.2.2 are composed mostly of two frequencies around 1010THz and 1250THz, corresponding to wavelengths of 297nm and 240nm, respectively. It is not clear why the oscillations occur at these exact frequencies, but detailed investigation is beyond the scope of this project.

Overall, it is clear that the device performs its task adequately, even though one of the key components could not be used. Further improvements of HHG efficiency can be expected if the polarizer glasses are cleaned well enough to be used with the device.

Chapter 5

Conclusions and outlook

5.1 Conclusions

An optical system for generating the second harmonic of a Ti:Sapphire laser pulse and controlling the polarization and delay between the fundamental and second harmonic pulses has been designed and modeled. Modeling results indicated that the system introduces little loss of pulse energy and that the polarization of the output pulses should be clean enough for the device to be of utility in performing $\omega + 2\omega$ high harmonic generation. Necessary components were acquired and the device was constructed.

Even-numbered high harmonics were successfully generated in argon, proving that the device performs according to expectations. Furthermore, overall HHG efficiency was not reduced much compared to generating high harmonics without the $\omega + 2\omega$ setup.

The final device will render very useful to obtain fine control on the process of high-order harmonic generation. The collinear device does not seem much inferior in functionality to an interferometric setup, but is much easier to use. Furthermore, it allows rapid and convenient switching between single-color and two-color HHG, whenever that is required by the application. Therefore, researchers will be able try more experiments in both single- and two-color modes.

After I had done most of the calculations, I accidentally found out about a commercial product from Eksma Optics[1] designed to perform similar functions (though for a different purpose - the Eksma device is a collinear third harmonic generator for Ti:Sapphire lasers). The components of the commercial device are a lot like those used in my setup, except that the commercial device does not include any means of cleaning the polarization (residual ellipticity is not harmful in that application) and uses a weaker delay compensation plate. Although the commercial device could not have been used for my task as is, knowing about it earlier would have reduced research time a lot. However, it was good to know that similar a device has been commercialized as it is an indication of the robustness of my design.

5.2 Self reflexion

The project involved an instructive insight into practical optics. During the course of the project, I had the opportunity to expand and refine my knowledge of fundamental optics, most notably the phenomenon of birefringence, as well as take a look at some of the more complex nonlinear optical phenomena. I expect this knowledge to be useful in my further studies and research.

5.3 Acknowledgments

First of all, I would like to express my gratitude to Anne L'Huillier for accepting me to into the Attosecond Physics group to do this project.

I am also grateful to almost every member of the Attosecond Physics group for various help during the course of the project, perhaps most notably Diego, Miguel and Esben.

Finally, my biggest thanks go to Cord for being a greatly supportive and inspiring project leader.

[1] http://www.eksmaoptics.com/en/search?product_id=&query=femtokit

Bibliography

[1] J. Mauritsson, P. Johnsson, E. Gustafsson, A. L'Huillier, K. Schafer, and M. Gaarde. Attosecond Pulse Trains Generated Using Two Color Laser Fields. *Physical Review Letters*, 97(1):1–4, July 2006.

[2] I Kim, Chul Kim, Hyung Kim, Gae Lee, Yong Lee, Ju Park, David Cho, and Chang Nam. Highly Efficient High-Harmonic Generation in an Orthogonally Polarized Two-Color Laser Field. *Physical Review Letters*, 94(24):2–5, June 2005.

[3] G. Lambert, F. Tissandier, J. Gautier, C. P. Hauri, P. Zeitoun, C. Valentin, T. Marchenko, J.-P. Goddet, M. Ribière, a. Sardinha, M. Fajardo, F. Hamouda, G. Maynard, G. Rey, and S. Sebban. Aberration-free high-harmonic source generated with a two-colour field. *EPL (Europhysics Letters)*, 89(2):24001, January 2010.

[4] Serge Huard. *Polarization of Light*. Wiley, Chinchester, 1997.

[5] Robert W. Boyd. *Nonlinear Optics*. Academic Press, 2 edition, 2003.

[6] Audrius Dubietis. *Netiesine optika*. Vilnius University Press, 2009.

[7] RC Jones. A new calculus for the treatment of optical systems. *JOSA*, 31:488–493, 1941.

[8] Edson R. Peck and Kaye Reeder. Dispersion of Air. *Journal of the Optical Society of America*, 62(8):958, August 1972.

[9] X. He, J. Dahlström, R. Rakowski, C. Heyl, A. Persson, J. Mauritsson, and Anne L'Huillier. Interference effects in two-color high-order harmonic generation. *Physical Review A*, 82(3):2–5, September 2010.